

Author version: *J. Oceanogr.*, vol.70(3); 2014; 307–321

Spectral wave characteristics off Gangavaram, Bay of Bengal

V. Sanil Kumar^{1*}, K. K. Dubhashi¹, T.M. Balakrishnan Nair²

¹CSIR-National Institute of Oceanography
(Council of Scientific & Industrial Research), Dona Paula, Goa 403 004 India

²Ocean Science & Information Services Group, Indian National Centre for Ocean Information System (Ministry of Earth Sciences), "Ocean Valley", Pragathi Nagar (BO), Nizampet (SO), Hyderabad - 500 090 India

*corresponding author Tel: 0091 832 2450 327 Fax: 0091 832 2450 602

email:sanil@nio.org URL: www.nio.org

Abstract

Spectral wave characteristics are studied based on waves measured for one year during 2010 off Gangavaram, Bay of Bengal. Maximum wave height of 5.2 m is observed on 19 May 2010 due to the influence of cyclonic storm LAILA. Wave spectrum is single-peaked during 57% of time and the double-peaked spectrum observed is predominantly swell dominated. Low-frequency waves (0.05-0.15 Hz) are predominantly from 150-180°, whereas high-frequency waves (>0.15 Hz) during November-January are mainly from 90-120° and during July and August are from 180-210°. Annual average significant wave height is similar to the value (1 m) observed in eastern Arabian Sea.

Key Words: Double-peaked spectra, wind-seas, swells, wind waves, mixed sea state, directional waves; cyclone, east coast of India

1. Introduction

Wave spectral parameters are required for planning marine operations and design of marine structures (Chakrabarti 2005). Waves in the ocean generally consist of locally generated waves and the swells propagating from far-off resulting in multi-peaked wave energy spectrum (Soares 1991; Hanson and Philips 1999). Kumar et al. (2003) found that along the Indian coast, about 60% of the wave spectra are multi-peaked and they are mainly single-peaked when the significant wave height (H_s) is more than 2 m. Rao and Baba (1996) observed multi-peaked wave spectra with energy of the wind-seas more than that of the swells off Goa (central west coast of India) at 80 m water depth during 17 to 24 March 1986. A number of semi-empirical spectral models are available for different conditions (Chakrabarti 2005). For a fully arisen sea condition, the Pierson-Moskowitz spectrum (Pierson and Moskowitz 1964) is used and for a growing sea state the JONSWAP spectrum (Hasselmann et al. 1973) is used. Dattatri et al. (1977), Narasimhan and Deo (1979), Baba et al. (1989) and Kumar et al. (1994), by analysing the data collected along the west coast of India recommended using the Scott spectrum (Scott 1965). Harish and Baba (1986) proposed PMK spectral model combining the Pierson-Moskowitz (1964) and Kitaigorodskii et al. (1975) spectra for the south-west coast of India. Kumar and Kumar (2008) studied the spectral characteristics of high ($H_s > 2$ m) shallow water waves and found that the measured wave spectrum can be represented by a JONSWAP spectrum with the modified JONSWAP parameters. Suresh et al. (2010) studied the wind-sea and swell characteristics off Visakhapatnam based on the southwest monsoon data (June-September 2009) and found that waves are mainly swells.

Along the east coast of India, the coast is exposed to seasonally reversing winds, with winds from the southwest (SW) direction during the southwest (summer) monsoon period (June to September) and from the northeast (NE) during the northeast (winter) monsoon period (October to January). The period between NE and SW monsoon is the pre-monsoon period or the fair weather (FW) period. The seasonal changes in winds produce similar changes in waves and the nature of the seasonal variability off the east coast of India is not described. The waters off east coast of India are also influenced by cyclones of the North Indian Ocean. Recently explorations in a number of nearshore and offshore oil and gas fields are proposed of the east coast of India. Hence, it is important to know the variations in wave spectral characteristics over a period of one year. Accordingly we studied the spectral characteristics of waves off Gangavaram in Bay of Bengal (Figure 1) based on one year measurements carried out using moored directional waverider buoy. During the study period, two cyclones (LAILA and JAL) developed in Bay of Bengal influenced the waves at the measurement

location and hence the wave characteristics during these cyclones are examined. Since directional spreading of sea states is an important design parameter, we have also examined the variation of directional spreading parameter. The measurement location is around 15 m water depth (geographic position 17.632° N; 83.265° E) and the distance of the location from the Indian subcontinent is 1.3 km and is 6 km southwest of Visakhapatnam (Figure 2). Tides in the region are mixed and are predominantly semi-diurnal and the average tidal range at Visakhapatnam, which is 6 km northeast of Gangavaram is 1.43 m during spring tide and 0.54 m during neap tide. Due to the low tidal range, the influence of tide on the waves will be marginal.

2. Materials and methods

Datawell directional waverider buoy (Barstow and Kollstad 1991) is used to measure waves during 1 January to 31 December 2010. The directional waverider buoy is a spherical case of 0.9 m diameter containing three accelerometers oriented orthogonally in one vertical and two horizontal directions. The vertical and horizontal (eastward and northward) displacements are obtained by double integration of the respective acceleration signal without applying filter. The displacement data are recorded continuously at 1.28 Hz and the data for every 30 minutes are processed as one record. Recorded time series is subjected to standard error checks for spikes, steepness and constant signals (Haver 1980) and a total of 17078 records are used for further analysis and it represents 97.5% of the time in the year 2010. FFT analyzed data from Datawell buoy processor are used (Datawell 2009). At every 200 s, a total number of 256 heave samples are collected and a Fast Fourier transform (FFT) is applied to obtain a periodogram in frequency range 0 to 0.58 Hz with frequency resolution of 0.005 Hz. The periodogram is smoothed using Hanning window with 25% overlap and the spectrum is obtained. Eight consecutive spectra covering 1600 s are averaged and used to compute the half-hourly wave spectrum. Significant wave height (H_s) and mean wave period (T_{m02}) are estimated from the spectral moment. Definitions of wave parameters used in the study are presented in Annexure. Period corresponding to the maximum spectral energy density, i.e., spectral peak period (T_p) is obtained from the wave spectrum. Mean wave direction (θ_m) and the directional width (σ) corresponding to the spectral peak are estimated based on circular moments (Kuik et al. 1988). Other parameters obtained are spectral peakedness parameter (Q_p) (Goda 1970), spectral narrowness parameter (ν) and the maximum spectral energy density (E_{max}). Zero-crossing analysis of the surface elevation time series is used to estimate maximum wave height (H_{max}) and wave period corresponding to H_{max} ($T_{H_{max}}$). The measurements are made in Coordinated Universal Time (UTC) and the time referred in the paper is in UTC. Wave age is estimated as C_p/U , where C_p is the wave

phase speed at peak frequency and U is wind speed. The wind-seas and swells from the measured wave data are separated through the proposed a 1-D separation algorithm (Portilla et al. 2009), on the basis of the assumption that, the energy at the peak frequency of a swell system cannot be higher than the value of a PM spectrum with the same peak frequency. It calculates the ratio (γ^*) between the peak energy of a wave system and the energy of a PM spectrum at the same frequency. If γ^* is above a threshold value of 1, the system is considered to represent wind-sea, else it is taken to be swell. Wind-sea and the swell parameters are computed by integrating over the respective spectral parts and are denoted with suffix 'w' and 's'. Reanalysis data of zonal and meridional components of wind speed at 10 m height based on model results (albeit assimilated) at 6 hour temporal resolution on approximately 2 degree grid from NCEP/NCAR (Kalnay et al. 1996) are used to study the seasonal change in wind pattern. These data are provided by the NOAA-CIRES Climate Diagnostics Center, Boulder, Colorado at <http://www.cdc.noaa.gov/>. Kumar and Sajiv (2010) compared the buoy measured wind data with the NCEP reanalysis data for a location 370 km south of the study area and found that the correlation coefficient varied from 0.68 to 0.84. The meteorological convention is used for presenting the wind and wave direction data (0 and 360° for wind/wave from North, 90 for East, 180 for South, 270 for West).

3. Results and discussions

3.1 Wave spectral parameters

During the one-year period, 54% of the time, H_s is less than 1 m and the 25th percentile of H_s is 0.7 m (Table 1). 25% of the time, H_s is more than 1.3 m and 0.2% of the time H_s exceed 2.5 m. H_s is less than 1.5 m during January to April (Figure 3b). The variation in wind-sea direction is similar to the wind direction (Figure 3a and 3c). During January, February and December, wind-sea direction is predominantly from the sector between 90 and 120°. During the study period, H_s up to 3 m and maximum wave height up to 5.2 m is observed on 19 May 2010 03 h. The high waves recorded in May are due to the cyclonic storm LAILA formed over southeast Bay of Bengal during 17-20 May 2010 (Figure 4a). Percentage of swell energy is higher than that of the wind-seas during the cyclone period (Figure 4b). The cyclone crossed the coast at 335 km SW of the wave measurement location between 11 and 12 h on 20 May 2010. Maximum wind speed of 27.5 m/s and the minimum sea level pressure of 98600 Pa are on 19 May 2010 when the cyclone is at 15° N and 81° E (350 km away from the wave measurement location). Due to the influence of cyclone, H_s increased from 1 to 3 m during 18 May 2010 11h to 19 May 2010 03 h and T_{m02} increased from 4 to 7 s (Figure 4c) and peak wave period shifted from 13.3 to 10 s (peak frequency shifted from low (0.075 Hz) to high (0.1

Hz)). Before the cyclone (during 15-17 May 2010), the waves are predominantly swells with H_s less than 1 m. During the cyclone due to increase in the locally generated waves, the peak frequency shifted towards the higher frequency. Before the cyclone (15-16 May 2010) the wind-seas are from $150-180^\circ$ and during the cyclone (18-19 May 2010) the wind-seas are from $60-150^\circ$ whereas the swells are constantly from 140 to 175° (Figure 4d). The wave spectra changed from broad to narrow band due to the cyclone and hence the spectral narrowness parameter reduced from 0.7 to 0.5 (Figure 4e). Wave spectra during 18-20 May 2010 shows the spectral narrowing due to shifting of spectral energy to a narrow range of frequencies (0.1 to 0.16 Hz) around the peak value (Figure 5). Multi-peaked spectrum observed is with a narrow swell and a broader wind-sea. Fluctuation of spectral narrowness parameter is similar to the fluctuation of ratio of mean period of swell and wind-sea (Figure 4f). It is also similar to the ratio of the swell height to wind-sea height. Before the cyclone, the average value of the ratio of T_{m02} of swell and wind-sea is more than 3 and during the cyclone this ratio reduced and varied between 2 and 2.5 indicating the increase in wave period of wind-sea and decrease in period of swell (Figure 4f). The reason for a higher ratio of T_{m02} of swell and wind-sea prior to the cyclone is that when the cyclone is further away the swells travel greater distances, and as they do they down shift the spectral energy due to non-linear interactions.

During the measurement period two more cyclonic storms developed in Bay of Bengal (GIRI during 20-23 October 2010 and JAL during 4-8 November 2010). Cyclone GIRI moved towards eastern part of Bay of Bengal and hence the wave characteristics did not change. During the cyclone JAL, H_s increased from 0.8 to 2.5 m during 6 November 2010 03 h -7 November 2010 03 h and H_{max} reached up to 4.8 m (Figure 6a). Percentage of swell energy is higher than the wind-seas during the cyclone period similar to the observation during cyclone LAILA (Figure 6b). Maximum wind speed of 30 m/s and the minimum sea level pressure of 98800 Pa are on 6 Nov 2010 when the cyclone JAL is at 11° N and 84° E. Increase in T_{m02} and change in peak frequency is similar to that observed during cyclone LAILA (Figure 6c). Before the cyclone, long period swells ($T_p > 10$ s) are observed and during the cyclone T_p is around 9-10 s. Being the NE monsoon period, the wind-sea before cyclone is from NE ($\theta_m < 150^\circ$) and during the cyclone wind-sea and swell are from same direction (Figure 6d). Variation of the spectral narrowness parameter is similar to that during cyclone LAILA (Figure 6e). The diurnal variation in wind-seas observed is due to the sea/land breeze influence with higher waves at 12:00 h (17:30 local time). As the wind-sea height increased, the spectral narrowness parameter reduced indicating the high waves are narrow banded. Higher wind-seas are from East than that from the southeast. Average value of the ratio of T_{m02} of swell and wind-sea is more than 2.5 and during the cyclone this ratio reduced and varied between 1.5 and 2.5 indicating the increase

in wave period of wind-sea and decrease in period of swell (Figure 6f). Influence of cyclone JAL on the waves off Gangavaram is relatively less than that due to cyclone LAILA since the track of JAL is 520 km away from the measurement location whereas the track of LAILA is at 335 km.

During the SW monsoon period, maximum Hs measured is 2.3 m and is slightly lower than the maximum value (2.6 m) reported for the year 2009 (Suresh et al. 2010). During NE monsoon period, the maximum Hs measured is 2.5 m and is due to the cyclone JAL. Kumar et al. (2004) measured maximum Hs of 3.29 m at 15 km southwest of the present study area during a cyclone in November 1998. Due to cyclones, high waves are observed during the FW and the NE monsoon period, but the average Hs is high (1.3 m) during the SW monsoon period (Table 2). Even though Bay of Bengal is more frequented by cyclones than Arabian Sea with ratio of the frequency as 4:1 (Dube et al. 1997), Hs is more than 2 m only during 1.8% of time in a year off Gangavaram, Bay of Bengal whereas along the Arabian Sea, 14-19% of the time Hs is more than 2 m (Kumar et al. 2014). Even though the maximum Hs is less than that (3.7 m) reported for the Arabian Sea for the same year 2010, the annual average value of Hs is similar (≈ 1 m) to the value for Arabian Sea (Sajiv et al. 2012) since the waves in Arabian Sea will be rough only during June to September (SW monsoon) whereas the waves in Bay of Bengal will be rough during May and November-December apart from June to September due to the cyclones and the influence of NE monsoon. In a year, Hs is more than 1 m during 45% of time in Bay of Bengal whereas it is 35% in Arabian Sea (Sajiv et al. 2012). 47% of the waves recorded are having spectral peak wave period between 6 and 12 s. High waves ($H_s > 2$ m) are having spectral peak period between 8 and 12 s and the long period swells (14-20 s) are having $H_s < 2$ m (Figures 7a to 7c). The average ratio of T_{m02} to T_p is 0.5 and that is much less than (0.78) that for wind-sea (Wolf et al. 2011) and the lower values are due to the predominance of swell at the measurement location. Significant steepness [$=2\pi H_s/(g T_{m02} T_{m02})$] varied from 1:18 to 1:262 with mean steepness of 1:58). Similar to Hs, the maximum spectral energy density is also high for waves with T_p ranging from 8 to 12 s (Figures 7d to 7f).

Since the wave spectra are multi-peaked consisting of swells and locally generated waves (wind-seas), the swell components and the wind-seas are separated and the wave parameters of wind-sea and swell are presented in Table 2. Average value of the ratio of the swell to wind-sea height is 1.3, 1.7 and 1.5 during FW, SW and NE monsoon period indicating predominance of swell in all the seasons. Average value of T_{m02} is slightly higher (6.2 s) during the SW monsoon period than that (5.2 s during FW and 5.4 s during NE) during other periods and the average of the mean wave period (T_{m02}) of wind-sea is 3.6 s and that of swell is 10.4 s (Table 2). Percentage of swells in the measured

data is 57, 65 and 59 during FW period, SW and NE monsoon period. During the same period, the percentage of swells along the west coast of India is 28, 74 and 33 (Glejin et al. 2013). For the study area, short period waves ($T_p < 6$ s; dominated by local seas) are less (4%) whereas the long period waves ($T_p > 12$ s; results primarily from swell) are high (62%). Waves with T_p more than 18 s are observed during 1.8% of time whereas along the west coast of India SW swells with $T_p > 18$ s are present for 3.6% of time (Kumar et al. 2014). Since the measurement is done in relatively shallow location (water depth ≈ 15 m), the measured waves are depth influenced. Average value of the ratio of water depth and wave length associated with the mean wave period is $0.3 < 0.5$ indicating that the measured waves are in the transitional water. Hence, the waves measured are the transformed waves and the wave height and the wave direction measured will be different from that in the deep water.

3.2 Wave spectra

The contour plots of normalized wave spectral energy density in frequency-time domain are presented to understand the evolution of spectral components over time (Figure 8a). During one year period, the wave spectral energy density varied from 0.02 to 13.5 m^2/Hz (Figure 9) and hence the normalization of each spectrum is carried out by dividing the wave spectral energy density by the corresponding maximum spectral energy density. During February and November-December, the spectral energy is spreading to higher frequencies (>0.25 Hz). During the SW monsoon period, 90% of the total spectral energy is within 0.05 to 0.25 Hz and only 5% of the total energy is spreading in frequencies greater than 0.3 Hz. Whereas during the FW and NE monsoon period, 14% of the spectral energy is between frequencies 0.3 and 0.58 Hz. Infra gravity waves (frequencies < 0.04 Hz) contribute to 0.2% of the wave heights. During the one-year period, single-peaked spectra are observed for 56.8% of time and the remaining are predominantly swell dominated (38.4%) double-peaked spectra and the wind-sea dominated double-peaked spectra observed is only 4.8%. The single-peaked spectra observed are similar (55 to 60%) to that reported for the waves at Frigg field, North Sea at 100 m water depth (Myrhaug and Slaattelid 1999). In North Atlantic 76% of the analyzed data are single-peaked during the storm period (Aranuvachapun 1987) and spectra with bimodal structure are about 20 to 25% in open North Sea and North Atlantic (Soares 1991). Chen et al. (2002) observed that swell occurs more than 80% of the time in most of the world's oceans and wind waves occur most frequently in the mid-latitudes, decreasing to a minimum at the equator. Chen et al. (2002) identified three "swell pools" in the tropics where the probability of swell is more than 95%. Wolf et al. (2011) found that waves in Liverpool Bay are mainly generated locally within the eastern Irish Sea so that long period swell is absent. Kumar et al. (2014) found large variation (46

to 63%) in the single-peaked spectra along the eastern Arabian Sea within a distance of 350 km due to the variation in local winds. In the present study, single-peaked spectra observed are high (73%) during May and September compared to other months (Table 3). During December and January, the wind-sea dominated double-peaked spectra are more (12%) compared to other months. Over an annual cycle only 4.8% of the spectra are wind-sea dominated (Table 3). During the SW monsoon period, the spectral peak is around 0.065 to 0.12 Hz (16 to 8 s) during 75% of the time whereas during the same period along the west coast of India, T_p varied in a narrow range (10 to 12 s) during 72% of the time (Glejin et al. 2012).

In order to know the predominance of wind-sea and swell, the monthly averaged wave spectrum is estimated (Figure 10). The peak wave period indicates that wave spectra are predominantly swell dominated in all the months. Monthly averaged wave spectrum is single-peaked during May, September and November primarily due to cyclonic activity and is double-peaked during remaining period. The wind-sea peaks are between 0.2 and 0.4 Hz from January-March, but lower in other times of the year indicating much younger seas during the former months. The secondary peak frequency of the swell dominated double-peaked spectra is at 1.1 to 5 times the primary peak frequency with an average value of 2.2 and is higher than the value (1.7) observed by Kumar et al. (2014) along the west coast of India. Baba et al. (1989) found multi-peaks at 1.5 to 2 times the peak frequency while analyzing the weekly collected data during February and June to September 1983 at 15 m water depth off south west coast of India. Annual average value of the difference between the spectral peaks is 0.10 Hz and the average ratio of the spectral energy at two peaks is 0.53. Kumar et al. (2003) found that the average value of the ratio of spectral energy of the two peaks as 0.6 and the average value of the difference between the peak frequencies as 0.09 Hz. Spectral peak period is more than 12 s during 49% of time and between 6 and 12 s during 47% of time. Waves having spectral peak period less than 6 s are observed only during 3.9% of time indicating the predominance of swell along the east coast of India. Waves having spectral peak period less than 5 s are not present during the SW monsoon period.

Kumar et al. (2014) found that spectral peakedness parameter (Q_p) is a good indicator for spectral narrowness. Present study also shows high values ($Q_p > 2$) for narrow band spectra (Figures 11a to 11c) and low values ($Q_p < 2$) for broad band spectra (Figures 11d to 11i). Q_p increases as the bandwidth becomes narrow (fully developed wind-seas have $Q_p \approx 2$, whereas narrow banded swells will have value >2). Goda (1976) has reported Q_p values of 2 to 3 from single-peaked spectra recorded in the Japanese coastal waters. For the study area, annual mean value of Q_p is 1.7 and for

high waves ($H_s > 2$ m) the average value of Q_p is 2.1. Q_p is very large for very narrow spectra (Figure 11c). For spectra with 75% of the spectral energy density within 0.05 Hz around the peak frequency, the Q_p values are higher than 2. For broad banded multi-peaked spectra, Q_p values observed for wind-sea dominated cases (Figure 11d and 11e) and for swell dominated case (Figure 11f) are similar. Kumar et al. (2010) found that during the onset of summer monsoon, the value of Q_p varied from 2.5 to 3. Since Q_p is a measure of spectral peakedness of a single-peaked spectrum, Q_p cannot be used as a measure of spectral peakedness for multi-peaked spectra.

Since the swell is a narrow spectrum, the JONSWAP spectrum (Hasselmann et al. 1973) with appropriate peak enhancement parameter (γ) can represent the swell (Goda 1983). Hence, Kumar and Kumar (2008) could represent the shallow water wave spectrum of high waves ($H_s > 2$ m) with JONSWAP spectrum with modified parameter. Furthermore, as swell results from a wind-sea that propagates away from the generation area, it is natural that a young swell is described by the same spectral model as wind-sea (JONSWAP). The study shows that single-peaked spectra of high waves ($H_s > 2$ m) could be represented with a fitted JONSWAP spectra (Figure 5). Fitted JONSWAP spectrum is obtained by selecting the parameter α (Phillips constant) and γ of the JONSWAP spectrum such that the peak of the spectrum agrees. The annual average value of the JONSWAP parameters, α and γ are 0.0014 and 1.31 (Table 4). Kumar and Kumar (2008) found that for waves with H_s more than 2 m, the estimated average value of the JONSWAP parameters, α and γ are 0.0027 and 1.63 and are less than the generally recommended values of 0.0081 and 3.3 respectively. Ochi and Hubble (1976) found that JONSWAP spectrum provided good approximation to the data for the uni-model spectra with JONSWAP parameters of $\alpha = 0.023$ and $\gamma = 2.2$. For high waves ($H_s > 2$ m), α and γ are 0.0027 and 1.64 and are close to the values reported by Kumar and Kumar (2008) and hence these values can be used for generation of theoretical wave spectra in design applications. In order to have a comparison between the measured and the theoretical spectra (fitted JONSWAP spectra), the spectral moments m_0 (zeroth) estimated from the theoretical spectrum are compared with that estimated from the measured data (Figure 12a). The correlation coefficient between the m_0 based on theoretical spectrum and measured spectrum is 0.85 for single-peaked spectra and is 0.68 for multi-peaked spectra. The correlation coefficient between the spectral estimates based on theoretical and measured are estimated and is presented in Figure 12b. For each spectrum, the root mean square error (RMSE) between the spectral estimates based on theoretical and measured is estimated. The average root mean square error (RMSE) between the spectral energy density estimate based on theoretical and measured is $0.42 \text{ m}^2/\text{Hz}$ for multi-peaked spectra and $0.21 \text{ m}^2/\text{Hz}$ for single-peaked spectra (Figure 12c). The RMSE between H_s computed based on JONSWAP spectra with

modified parameters and the measured data is 0.38 m for multi-peaked spectra and 0.29 m for single-peaked spectra. The study shows that JONSWAP spectra with modified parameters represent the measured single-peaked spectra well.

3.3 Wave direction

Low frequency waves (0.05-0.15 Hz) are predominantly from 150-180° (Figure 8b). High frequency waves (>0.15 Hz) during November-December and January are mainly from 90-120° due to the influence of NE monsoon and during July and August are from 180-210° due to the SW monsoon. The average of the mean wave direction during FW period and NE monsoon is the same (153°) and that during SW monsoon is 159°. The waves with T_p less than 6 s are predominantly from 180 to 225° during FW period and SW monsoon (Figures 7g and 7h) and are from 70 to 100° during NE monsoon period (Figure 7i). Waves with 6-18 s T_p are from 135-180° in all the seasons. Swells are predominantly from the sector between east and south with an average value of 155° (Table 2). The average directions of wind-seas are 167 and 176° during the FW and SW monsoon whereas during the NE monsoon period wind-seas are from 131°. The average difference in wave direction of wind-sea and swell varied from 15 to 26°. The monthly average mean wave direction of 0.1 Hz waves is nearly same ($\approx 155^\circ$) in all months whereas the direction of the waves having frequency 0.2 to 0.4 Hz are varying due to change in local wind pattern and due to the SW and NE monsoon winds (Figure 10). The 20 m depth contour at the measurement location is 45° to the east from the true north. Hence, waves having direction 135° will be approaching perpendicular to the coast and will not generate longshore current and littoral drift. Wave direction less than 135° will generate longshore currents and littoral drift towards SW and waves with direction more than 135° will generate longshore currents and littoral drift towards NE. Due to the NE monsoon winds, during November-December and January, direction of high frequency waves (0.2 to 0.4 Hz) is less than 135°. Whereas during the remaining period, direction of high frequency waves is more than 135°.

The directional spreading parameter (directional width) at spectral peak for high waves ($H_s > 2$ m) is less with average value of 19° compared to the annual average of 24°. The directional width is smallest at the peak of the spectrum and increases at frequencies lower than the peak and at frequencies higher than the peak (Figure 10). Increase in directional width being gradual for higher frequencies and higher for the lower frequencies is probably related to the lower frequency waves being narrow banded (in frequency). As a result the increase in spread is happening because the spectral energy is rapidly decreasing. Monthly average directional width at spectral peak is less

during May (21°) and July (23°) since during these months the waves are swell dominated ones which have a much narrower spread (Figure 3b).

3.4 Wind wave parameters

The inverse wave age, the ratio of the surface wind speed (U) to the speed of the waves at the peak of the spectrum (C_p) is a good indicator of the degree of coupling between the wind and the waves with higher the inverse wave age, the more strongly the waves are coupled to the wind. High values of inverse wave age indicate regions where the waves are strongly coupled to the local wind field and low values indicate regions where swells are present (Hanley et al. 2010). The average value of the inverse wave age for the study area is 0.56 indicating presence of swell driven wave regime (Hanley et al. 2010). Donelan et al. (1993) proposed that $U/C_p = 0.83$ corresponds to the value of the spectrum at full development, where the spectral components below this value is classified as swell and above as wind-sea. In the present case, 18% of the waves during the one-year period have inverse wave age more than 0.83 indicating that the pure wind-sea is less along the Bay of Bengal since the area is dominated by swells and the winds are weak in general (except SW monsoon period). During the SW monsoon period, 30% of the waves are having inverse wave age more than 0.83 due to the strong local winds. Based on data from five field campaigns to study the influence of wave age on the air-sea momentum flux during pure wind-sea conditions, Drennan et al. (2003) found that pure wind-seas are frequent in coastal regions, in enclosed seas, and during extreme wind events; however, in the open ocean swell is usually present. During 46% of the time in a year, locally generated waves [according to Thompson et al. (1984), wave steepness (H_s/L) > 0.025] are observed, but wave age of the measured data is less than 10 during 99% of time indicating that the waves are young sea with presence of swells.

4. Conclusions

The variations in wave spectral characteristics are studied for the first time off Gangavaram, a shallow water location in the Bay of Bengal using measured collected over a period of one year at an interval of 30 minutes. The study shows that high waves ($H_s > 2$ m) are with spectral peak period between 8 and 12 s and the long period swells (14-20 s) are with $H_s < 2$ m. Predominance of swells are observed in all the seasons and pure wind-seas are less since the area is dominated by swells and the winds are weak in general (except SW monsoon period). During the SW monsoon period, 90% of the total spectral energy is within 0.05 to 0.25 Hz and only 5% of the total energy is spreading in frequencies greater than 0.3 Hz. Whereas during the FW and NE monsoon period, 14% of the

spectral energy is between frequencies 0.3 and 0.58 Hz. During the one-year period, single-peaked spectra observed are 56.8% and the remaining are predominantly swell dominated (38.4%) double-peaked spectra. The secondary peak frequency of the swell dominated double-peaked spectra is at 1.1 to 5 times the primary peak frequency with an average value of 2.2 and is higher than the value (1.7) observed along the eastern Arabian Sea. Monthly averaged wave spectrum is single-peaked during May, September and November primarily due to cyclonic activity and double-peaked during remaining period. The wind-sea peaks are between 0.2 - 0.4 Hz from January-March, but lower in other times of the year indicating much younger seas during the former months. Due to the NE monsoon winds, the direction of high frequency (0.2 to 0.4 Hz) waves shifts from the west to the east of the shore normal during November-December and January. Bay of Bengal is frequented by cyclones and due to the influence of cyclonic storm LAILA passed 335 km SW of the wave measurement location, Hs up to 3 m and maximum wave height up to 5.2 m are observed. Percentage of swell energy is higher than that of the seas even during the cyclone period. Even though the annual maximum Hs is less than that reported for the eastern Arabian Sea, the annual average value of Hs is similar (≈ 1 m) to the value for Arabian Sea since the Bay of Bengal is rough during most of the time compared to Arabian Sea.

Acknowledgments

The authors gratefully acknowledge the financial support given by the Earth System Science Organization, Ministry of Earth Sciences, Government of India to conduct this research. The directors of CSIR-NIO, Goa and INCOIS, Hyderabad provided encouragement to carry out the study. We thank Mr. Arun Nherakkol, Scientist, INCOIS and NIO colleagues Dr. B.P. Rao, Mr. N.S.N. Raju and Mr. Jai Singh for the help during data collection. Mr. Glejin Johnson, Research Scholar, CSIR-NIO prepared Figure 1. Gangavaram Port officials and Andhra University provided the logistics during data collection period. We thank the two anonymous reviewers for critical comments and suggestions which improved the quality of the paper. This work is NIO contribution No. ****.

Annexure: Definition of wave parameters used in the study

$$\text{Significant wave height (Hs)} = 4\sqrt{m_0} \quad (\text{A1})$$

$$\text{Mean wave period (Tm}_{02}) = \sqrt{m_0/m_2} \quad (\text{A2})$$

$$\text{Spectral narrowness parameter (v)} = \sqrt{\frac{m_2 m_3}{m_1^2} - 1} \quad (\text{A3})$$

$$\text{Spectral peakedness parameter (Qp)} = \frac{2}{m_0^2} \int_0^\infty f S^2(f) df \quad (\text{A4})$$

Where m_n is the n th order spectral moment and is given by,

$$m_n = \int_0^\infty f^n S(f) df, \quad n=0, 1, 2 \text{ and } 4$$

$S(f)$ is the spectral energy density at frequency f .

References

- Aranuvachapun S (1987) Parameters of JONSWAP spectral model for surface gravity waves-I. Monte Carlo simulation study, *Ocean Eng* 14:89-115
- Baba M, Dattatri J, Abraham S (1989) Ocean wave spectra off Cochin, west coast of India, *Indian J Mar Sci* 18:106-112
- Barstow SB, Kollstad T (1991) Field trials of the directional waverider, *Proceedings of the First International Offshore and Polar Engineering Conference III*: 55-63
- Chakrabarti SK (2005) *Handbook of Offshore Engineering, Vol-1, Ocean Engineering Series, Elsevier*, pp. 661
- Chen G, Chapron B, Ezraty R, Vandemark D (2002) A global view of swell and wind sea climate in the ocean by satellite altimeter and scatterometer. *J Atmos Ocean Tech* 19:1849–1859
- Datawell (2009) *Datawell Waverider Reference Manual*. Datawell BV oceanographic instruments, The Netherlands, Oct. 10, pp.123
- Dattatri J, Jothi Shankar N, Raman H (1977) Comparison of Scott spectra with ocean wave spectra. *J Waterways Port Coastal and Ocean Eng ASCE* 103:375-378
- Donelan MA, Dobsen F, Smith S, Anderson R (1993) On the dependence of sea surface roughness on wave development. *J Phys Oceanogr* 23:2143–2149
- Drennan WM, Graber HC, Hauser D, Quentin C (2003) On the wave age dependence of wind stress over pure wind seas. *J Geophys Res* 108 8062. doi:10.1029/2000JC000715

- Dube SK, Rao AD, Sinha PC, Murty TS, Bahulayan N (1997) Storm surge in the Bay of Bengal and Arabian Sea: the problem and its prediction. *Mausam* 48:283–304
- Glejin J, Kumar VS, Nair TMB, Singh J (2013) Influence of winds on temporally varying short and long period gravity waves in the near shore regions of eastern Arabian Sea, *Ocean Sci* 9: 343–353.
- Glejin J, Kumar VS, Philip CS, Singh J, Pednekar P, Kumar KA, Dora UG, Gowthaman R (2012) Variations in swells along eastern Arabian Sea during the summer monsoon. *Open J Mar Sci* 2:43-50
- Goda Y (1970) Numerical experiments on wave statistics with spectral simulation, in: Report Port and Harbour Research Institute. *Japan* 9:3–57
- Goda Y (1976) “On Wave Groups,” Proc. Conf. Behaviour of Offshore Structures, Trondheim, Norway Vol. 1:115-128
- Goda Y (1983) Analysis of wave grouping and spectra of long-travelled swell. *Japan: Rep. Port Harbour Res. Inst.* 22: pp. 3-41
- Hanley KE, Belcher SE, Sullivan PP (2010) A global climatology of wind–wave interaction. *J Phys Oceanogr* 40:1263–1282
- Hanson J L, Phillips OM (1999) Wind sea growth and dissipation in the open ocean. *J Phys Oceanogr* 29: 1633-1648.
- Harish CM, Baba M (1986) Spectral and statistical properties of shallow water waves. *Ocean Eng* 13:239-248
- Hasselmann K, Barnett TP, Bouws E, Carlson H, Cartwright DE, Enke K, Ewing JA, Gienapp H, Hasselmann DE, Kruseman P, Meerburg A, Muller P, Olbers DJ, Richter K, Sell W, Walden H (1973) Measurements of wind-wave growth and swell decay during the Joint North Sea Wave Project (JONSWAP). *Deutsche Hydrograph. Z.* A12,95
- Haver S (1980) Analysis of uncertainties related to the stochastic modelling of ocean waves. Division of Marine structures, The Norwegian Institute of Technology, Norway, Report No. UR-80-09, pp. 187
- Kalnay E, Kanamitsu M, Kistler R, Collins W, Deaven D, Gandin L, Iredell M, Saha S, White G, Woollen J, Zhu Y, Leetmaa A, Reynolds B, Chelliah M, Ebisuzaki W, Higgins W, Janowiak J, Mo KC, Ropelewski C, Wang J, Roy Jenne, Joseph D (1996) The NCEP/NCAR 40-year reanalysis project. *Bulletin of the American Meteorological Society* 77:437-471
- Kitaigorodskii SA, Krasitskii VP, Zaslavskii MM (1975) On Phillips theory of equilibrium range in the spectra of wind generated gravity waves. *J Phys Oceanogr* 5:410-420
- Kuik AJ, Vledder G, Holthuijsen LH (1988) A method for the routine analysis of pitch and roll buoy wave data. *J Phys Oceanogr* 18:1020–1034
- Kumar VS, Anand NM, Kumar KA, Mandal S (2003) Multi-peakedness and groupiness of shallow water waves along Indian coast. *J Coastal Res* 19:1052-1065
- Kumar VS, Kumar KA (2008) Spectral representation of high shallow water waves. *Ocean Eng* 35:900-911

Kumar VS, Kumar KA, Raju NSN (2004) Wave characteristics off Visakhapatnam coast during a cyclone, *Current Science* 86(11):1524-1529

Kumar VS, Mandal S, Anand NM, Nayak BU (1994) Spectral representation of measured shallow water waves. *Proc. Indian National Conference on Harbour and Ocean Engg. (INCHOE-94)*, CWPRS, Pune India Vol. I: 23-32

Kumar VS, Sajiv P (2010) Variations in long term wind speed during different decades in Arabian Sea and Bay of Bengal, *Journal of Earth Systems Science* 119(5): 639-653

Kumar VS, Shanas PR, Dubhashi KK (2014) Shallow water wave spectral characteristics along the eastern Arabian Sea, *Natural Hazards* 70: 377-394 DOI 10.1007/s11069-013-0815-7.

Myrhaug D, Slaattelid OH (1999) Statistical properties of successive wave periods. *J offshore mechanics and Arctic Engineering* 121:166-177

Narasimhan S, Deo MC (1979) Spectral analysis of ocean waves - A study. *Proc. conf. Civil Engineering in Oceans*, ASCE 877-892

Ochi MK, Hubble EN (1976) On six parameter wave spectra. In *proceedings 15th Coastal Engineering Conference*, ASCE 321-328

Pierson WJ, Moskowitz L (1964) A proposed form for fully developed seas based on the similarity theory of S.A. Kitaigorodski. *J Geophys Res* 69:5181-5190

Portilla J, Ocampo-Torres FJ, Monbaliu J (2009) Spectral Partitioning and Identification of Wind Sea and Swell. *J Atmos Ocean Tech* 26:pp. 117-122

Rao CVKP, Baba M (1996) Observed wave characteristics during growth and decay: a case study. *Continental Shelf Res* 16(12): 1509-1520

Sajiv PC, Kumar VS, Johnson G, Dora, GU, Vinayaraj P (2012), Interannual and seasonal variations in nearshore wave characteristics off Honnavar, west coast of India, *Current Science* 103 (3): 286-292

Scott JR (1965) A sea spectrum for model test and long-term ship prediction. *J Ship Res* 9:145-152

Soares CG (1991) On the occurrence of double peaked wave spectra. *Ocean Eng.* 18(1/2):167-171

Suresh RRV, Annapurnaiah K, Reddy KG, Lakshmi TN, Balakrishnan Nair TM (2010) Wind sea and Swell Characteristics off East coast of India During Southwest Monsoon, *International Journal of Oceans and Oceanography* 4:35-44.

Thompson TS, Nelson AR, Sedivy DG (1984) Wave group anatomy. in: *Proceeding of 19th conference on Coastal engineering*, American Society of Civil Engineers, 1, 661-677

Wolf J, Brown JM, Howarth MJ (2011) The wave climate of Liverpool Bay—observations and modelling. *Ocean Dyn* 61:639-655

Figure Captions

Figure 1. Study area showing the location of wave measurement near Visakhapatnam. Gangavaram is 6 km southwest of Visakhapatnam

Figure 2. The depth contours near the wave measurement location

Figure 3. Variation of (a) wind speed and direction (b) significant wave height (c) direction of wind-sea and swell during 2010

Figure 4. Time series plot of (a) significant wave height and maximum wave height (b) significant wave height due to wind-sea and swell (c) mean wave period, peak wave period and period corresponding to Hmax (d) direction of swell and wind-sea (e) spectral narrowness parameter and (f) ratio of mean period of swell and wind-sea during cyclone LAILA

Figure 6. Wave spectra based on measurement and the fitted JONSWAP spectra during 18-20 May 2010, the period which waves are relatively high due to the influence of cyclone LAILA

Figure 6. Time series plot of (a) significant wave height and maximum wave height (b) significant wave height due to wind-sea and swell (c) mean wave period, peak wave period and period corresponding to Hmax (d) direction of swell and wind-sea (e) spectral narrowness parameter and (f) ratio of mean period of swell and sea during cyclone JAL

Figure 7. Variation significant wave height, maximum spectral energy density and mean wave direction with peak wave period during FW period (a, d and g), SW (b, e and h) and NE monsoon period (c, f and i)

Figure 8. Contour plots of (a) normalized spectral energy density and (b) mean wave direction during 2010. The white patch indicate the gap in the data

Figure 9. Time history of maximum spectral energy density during 2010

Figure 10. Monthly averaged wave spectra (solid line), mean wave direction (dashed line) and directional width (dotted line) in different months

Figure 11. Typical single and multi-peaked wave spectra recorded

Figure 12. (a) Variation of zeroth spectral moment estimated based on measured and theoretical spectra and (b) variation of correlation coefficient between measured and theoretical spectra with significant wave height

Table 1. Percentage of occurrence and exceedance of waves

Significant wave height (m)	Number of occurrence	Percentage of occurrence	Percentage of exceedance
0.0 - 0.5	1411	8.26	91.74
0.5 - 1.0	7796	45.65	46.09
1.0 - 1.5	5395	31.59	14.50
1.5 - 2.0	2166	12.68	1.82
2.0 - 2.5	276	1.62	0.20
2.5 - 3.0	32	0.19	0.01
3.0 - 3.5	2	0.01	0.00

Table 2. Average value of wave parameters during 2010

Parameter	FW period (Pre monsoon)	SW monsoon	NE monsoon
Hs (m)	0.86	1.3	0.83
Hmax (m)	1.3	2.0	1.3
Hs _s (m)	0.65	1.0	0.62
Hs _w (m)	0.54	0.77	0.51
Tm ₀₂ (s)	5.2	6.2	5.4
Tm _{02s} (s)	10.8	10.3	10.2
Tm _{02w} (s)	3.4	3.9	3.5
Tp (s)	11.9	12.6	11.2
θ _m (deg)	153	159	153
θ _{ms} (deg)	152	157	157
θ _{mw} (deg)	167	176	131
σ (deg)	23.3	21.1	26.6
v	0.63	0.57	0.61
Qp	1.7	1.6	1.8
U/Cp	0.57	0.70	0.45
E _{max} (m ² /Hz)	1.1	2.2	0.91
Swell to wind-sea height (Hs _s /Hs _w)	1.3	1.7	1.5
Swell (%)	57	65	59
Wind-sea (%)	43	35	41

Table 3. Percentage of single-peaked, swell and wind-sea dominated double-peaked spectra

Month	Single-peaked spectra	Double-peaked spectra	
		Swell dominated	Wind-sea dominated
January	50.7	37.7	11.6
February	58.3	36.6	5.1
March	51.2	41.0	7.8
April	45.3	51.5	3.2
May	73.3	24.5	2.2
June	45.1	54.1	0.8
July	42.5	49.1	8.4
August	56.3	41.8	1.9
September	73.1	26.5	0.4
October	72.0	27.4	0.6
November	57.4	39.2	3.4
December	53.3	35.0	11.7
Full year	56.8	38.4	4.8

Table 4. Monthly average value of significant wave height, mean wave period and JONSWP parameters

Month	Significant wave height (m)	Mean wave period (s)	Peak enhancement parameter, γ	Phillips constant, α
January	0.7	7.6	1.37	0.0016
February	0.5	6.4	1.62	0.0027
march	0.8	9.0	1.47	0.0021
April	1.0	10.9	1.14	0.0007
May	1.4	9.9	1.30	0.0014
June	1.5	10.0	1.38	0.0017
July	1.5	10.6	1.35	0.0016
August	1.4	11.9	1.21	0.0010
September	1.4	11.3	1.21	0.0010
October	1.1	9.7	1.22	0.0010
November	1.1	9.2	1.33	0.0015
December	1.0	8.9	1.37	0.0016
Full year	1.0	5.6	1.31	0.0014

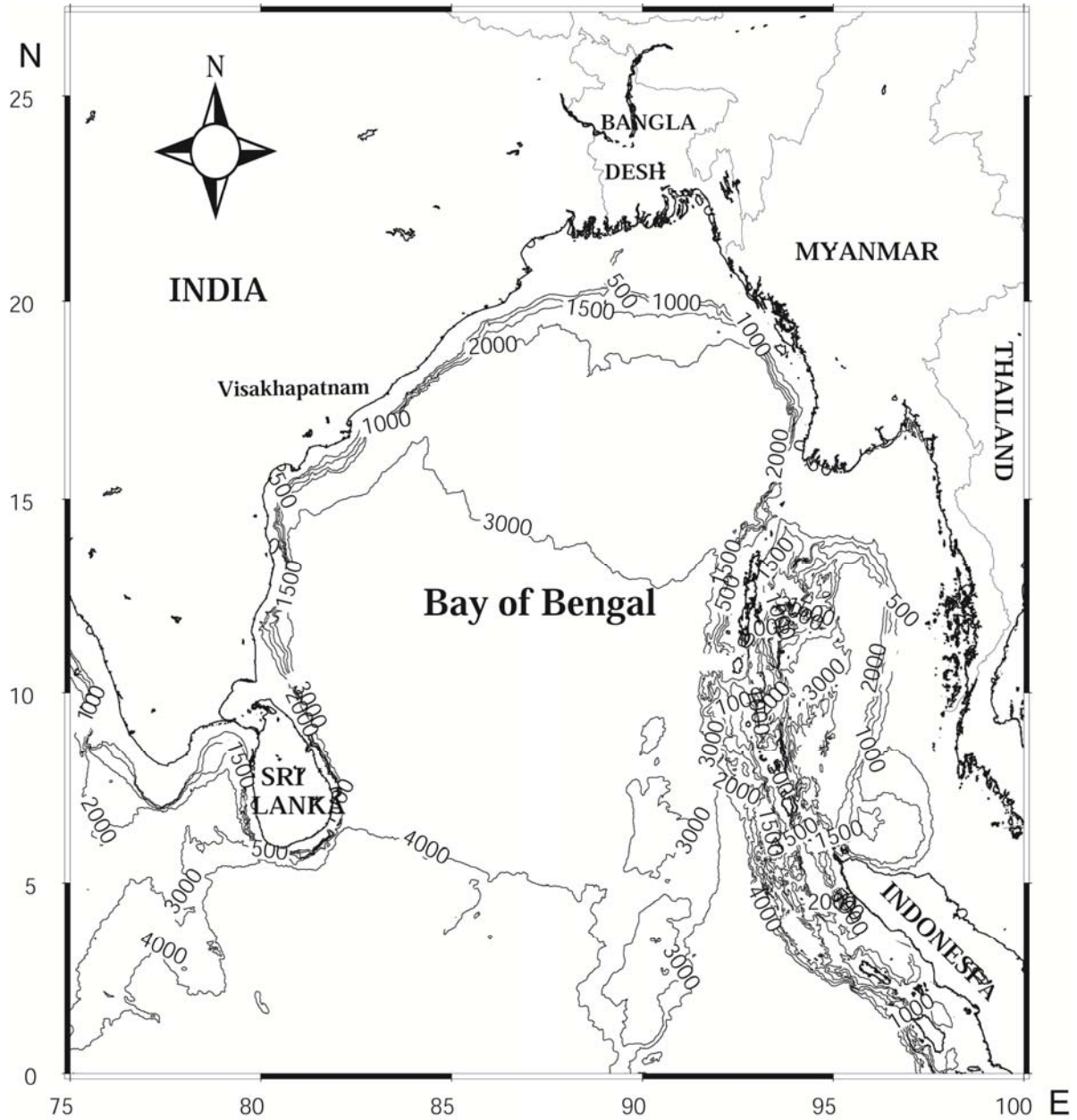


Figure 1 Study area showing the location of wave measurement near Visakhapatnam. Gangavaram is 6 km southwest of Visakhapatnam

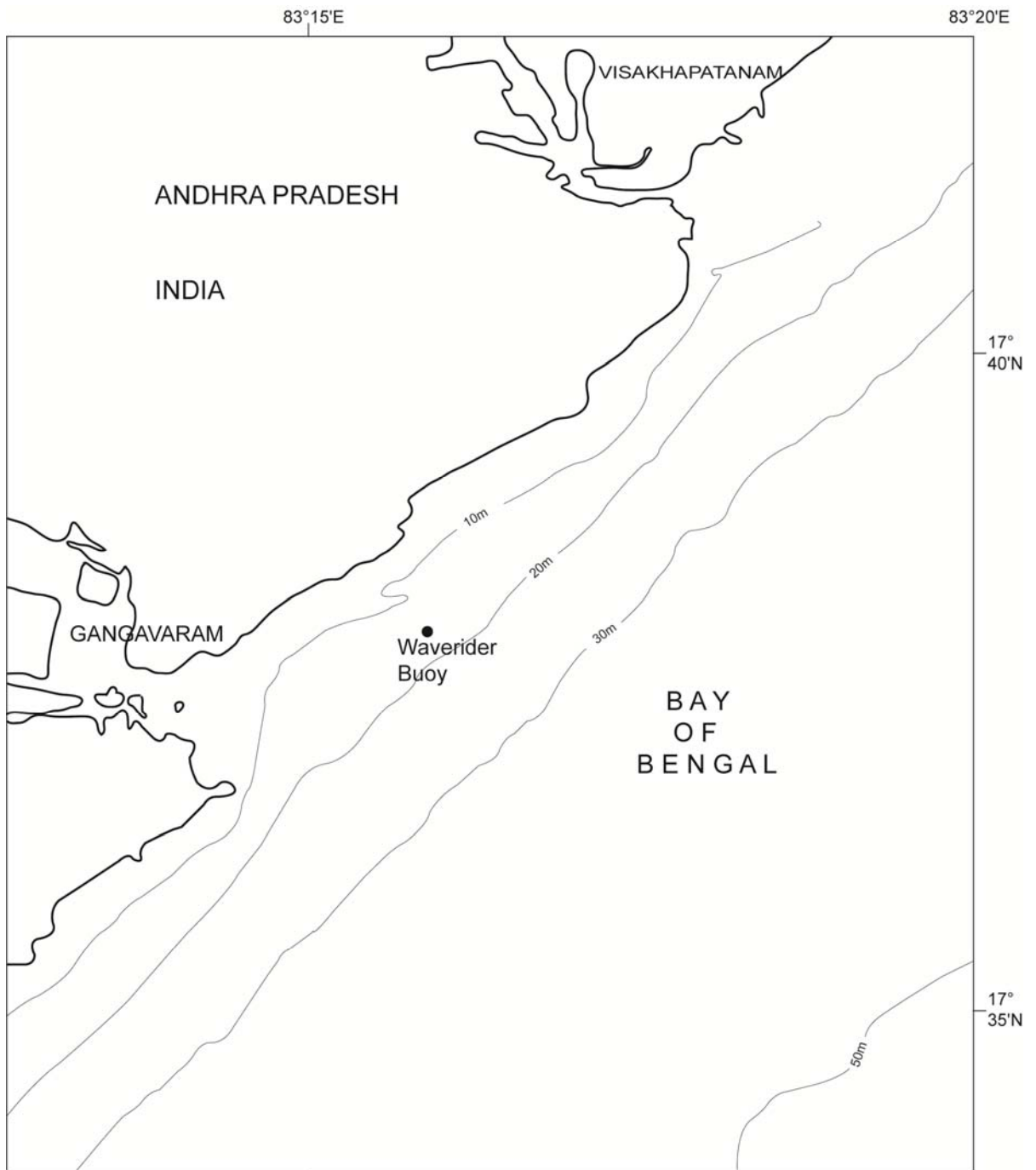


Figure 2 The depth contours near the wave measurement location

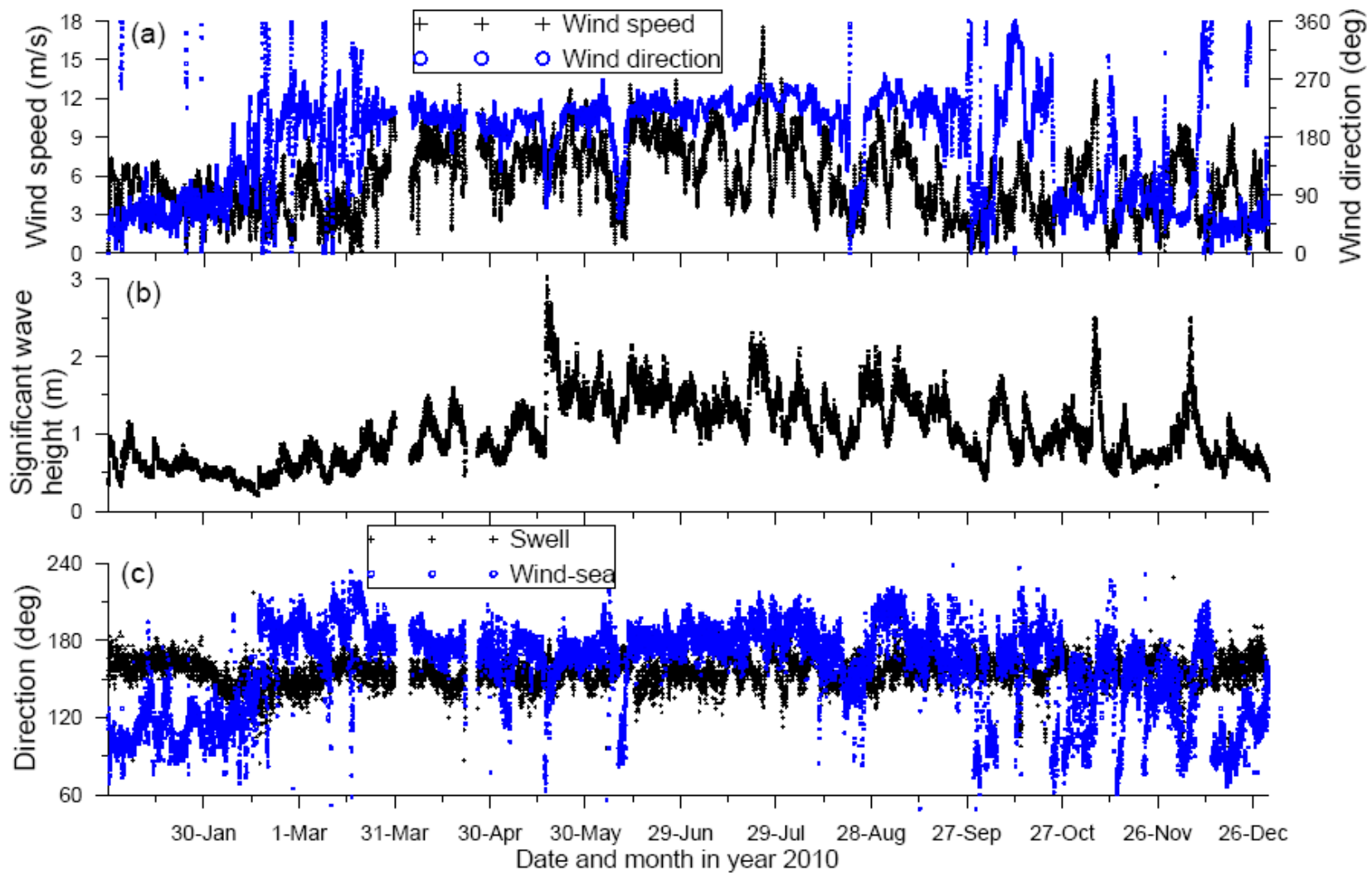


Figure 3. Variation of (a) wind speed and direction (b) significant wave height (c) direction of wind-sea and swell during 2010

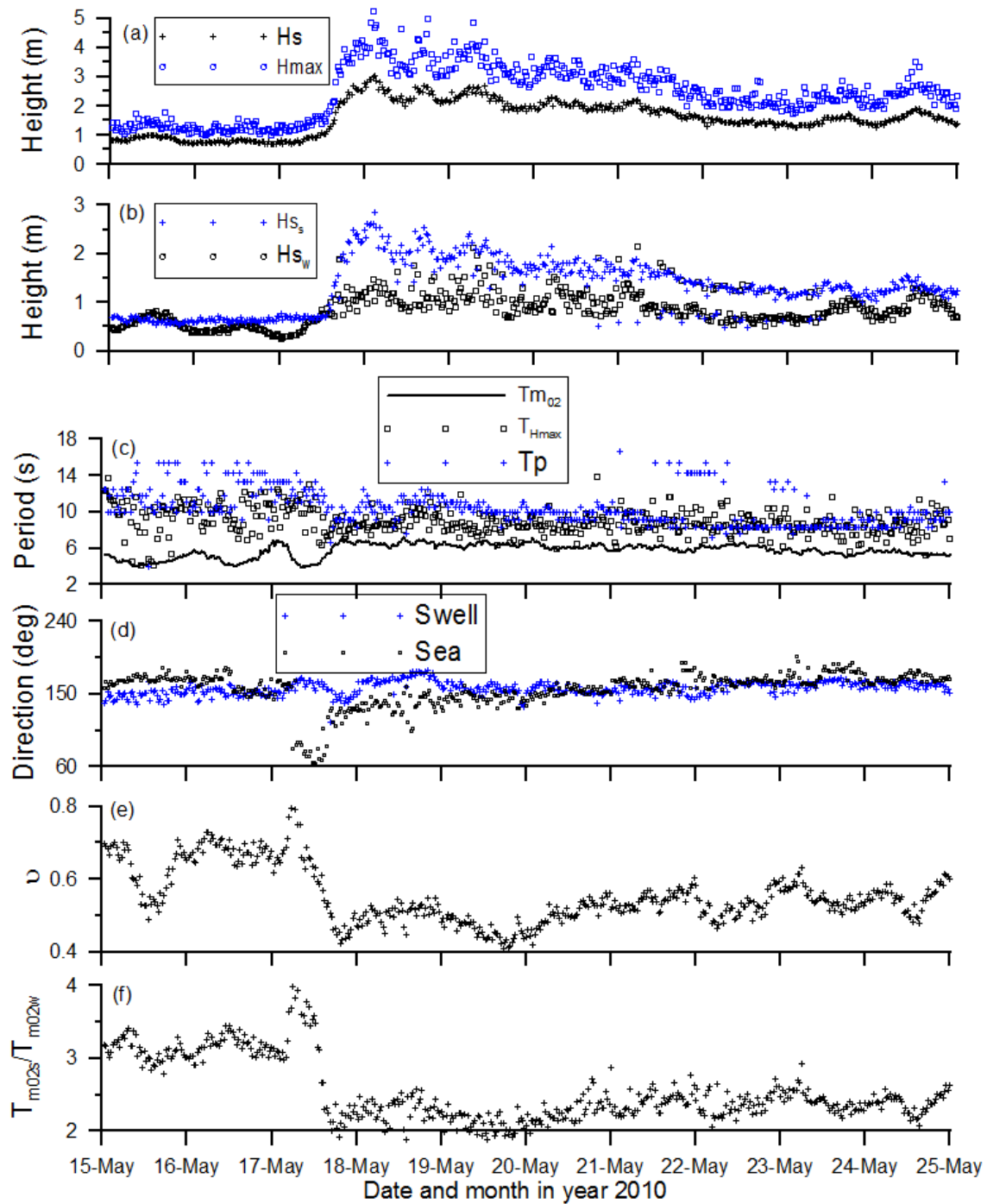


Figure 4. Time series plot of (a) significant wave height and maximum wave height (b) significant wave height due to wind-sea and swell (c) mean wave period, peak wave period and period corresponding to Hmax (d) direction of swell and wind-sea (e) spectral narrowness parameter and (f) ratio of mean period of swell and wind-sea during cyclone LAILA

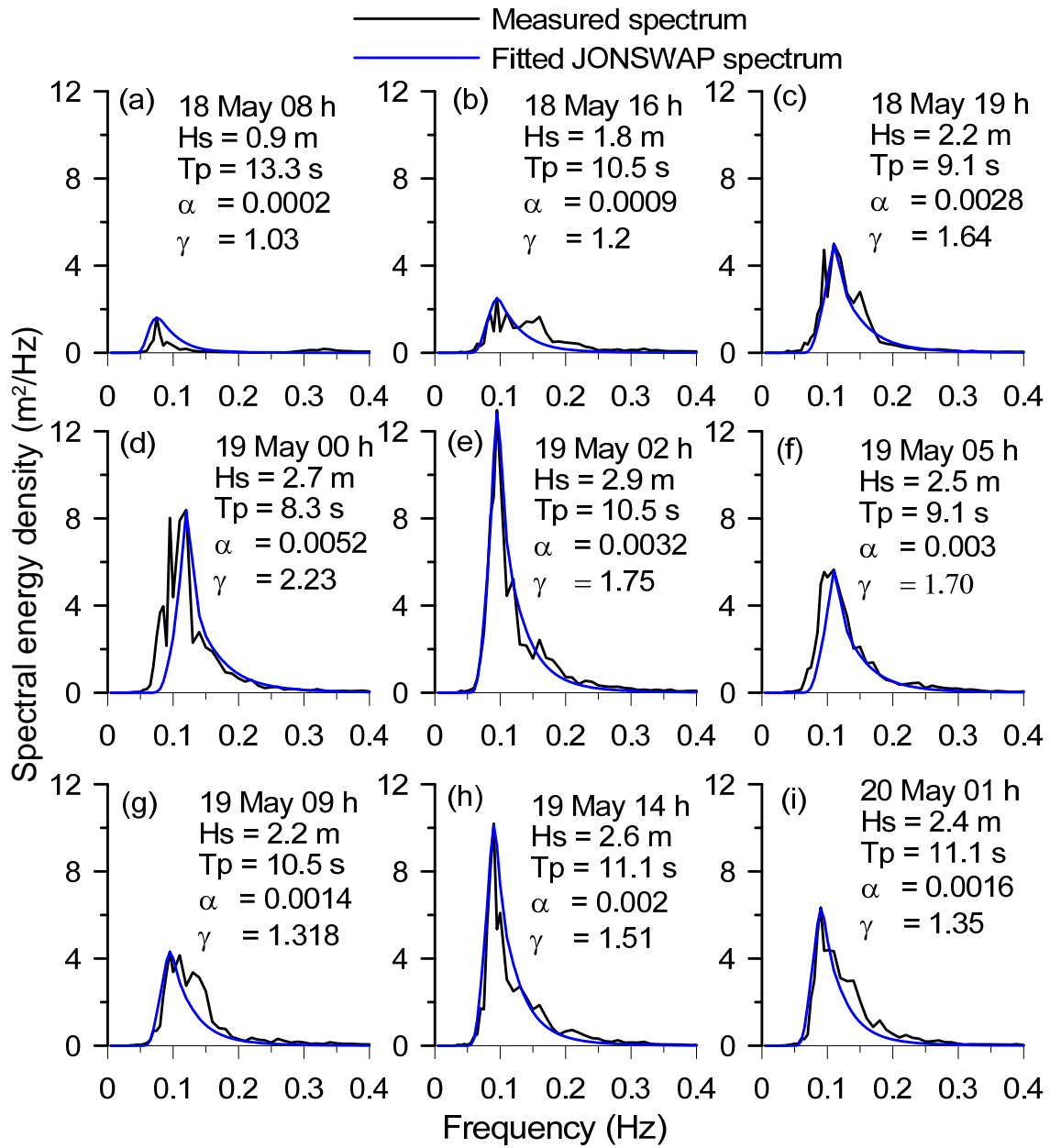


Figure 5. Wave spectra based on measurement and the fitted JONSWAP spectra during 18-20 May 2010, the period which waves are relatively high due to the influence of cyclone LAILA

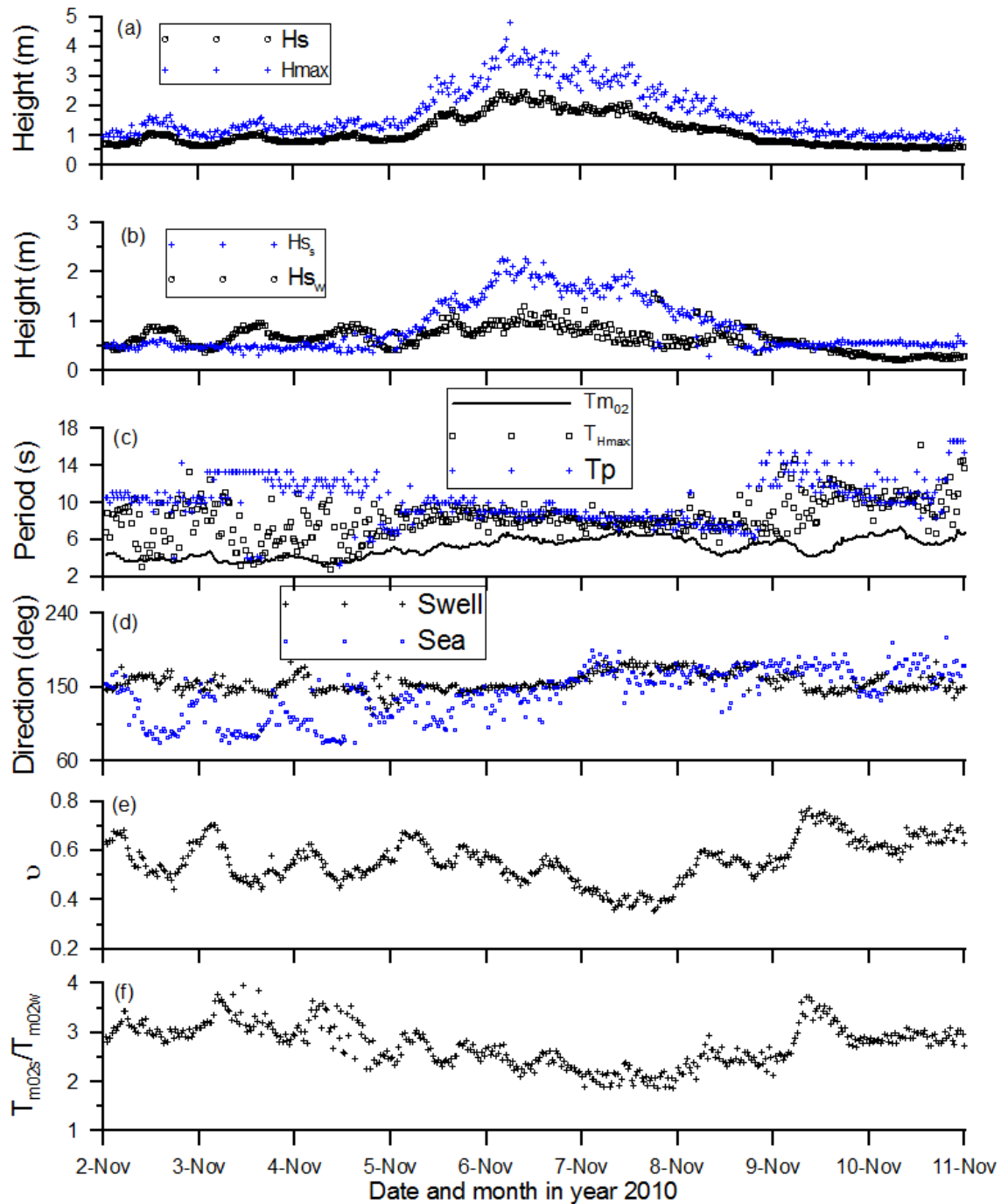


Figure 6. Time series plot of (a) significant wave height and maximum wave height (b) significant wave height due to wind-sea and swell (c) mean wave period, peak wave period and period corresponding to Hmax (d) direction of swell and wind-sea (e) spectral narrowness parameter and (f) ratio of mean period of swell and wind-sea during cyclone JAL

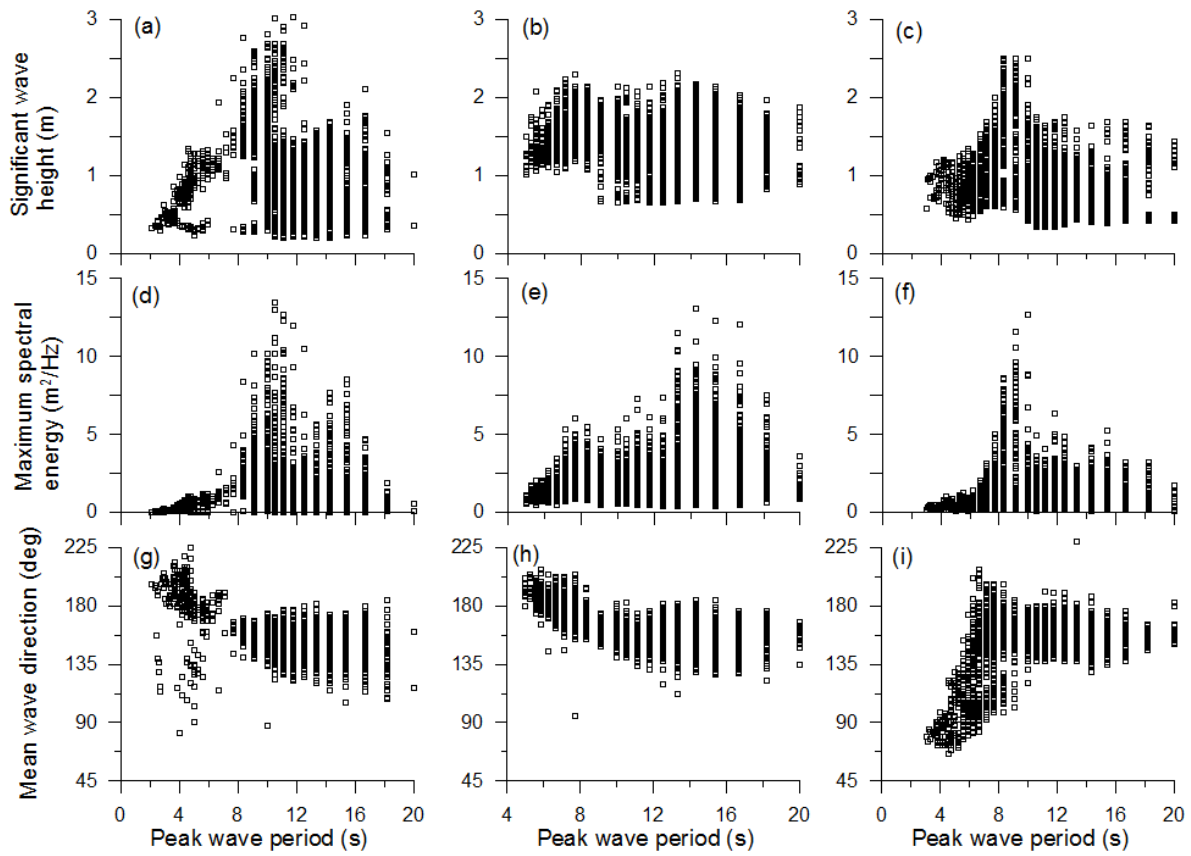


Figure 7. Variation significant wave height, maximum spectral energy density and mean wave direction with peak wave period during FW period (a, d and g), SW (b, e and h) and NE monsoon period (c, f and i)

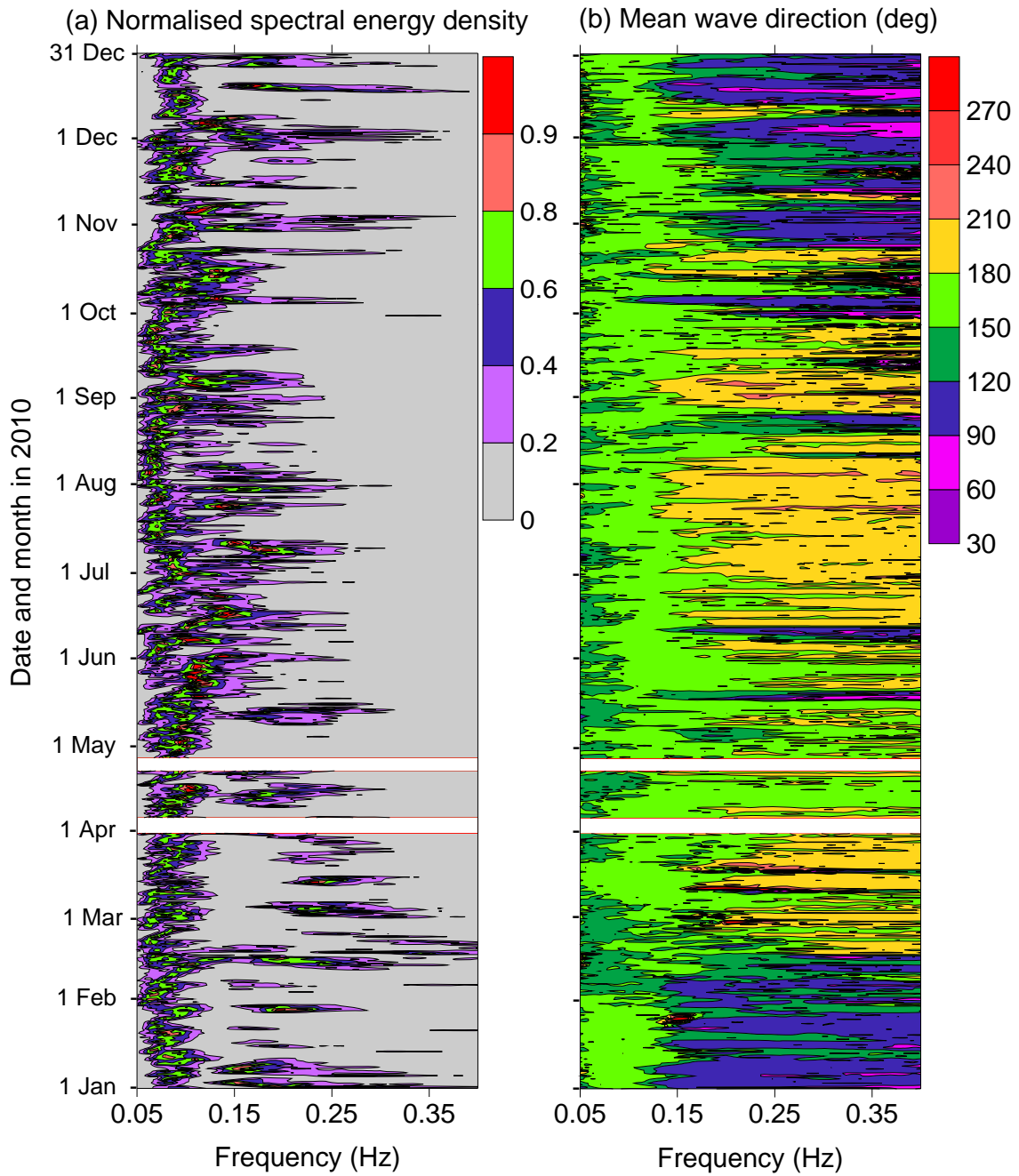


Figure 8 Contour plots of (a) normalized spectral energy density and (b) mean wave direction during 2010. The white patch indicate the gap in the data

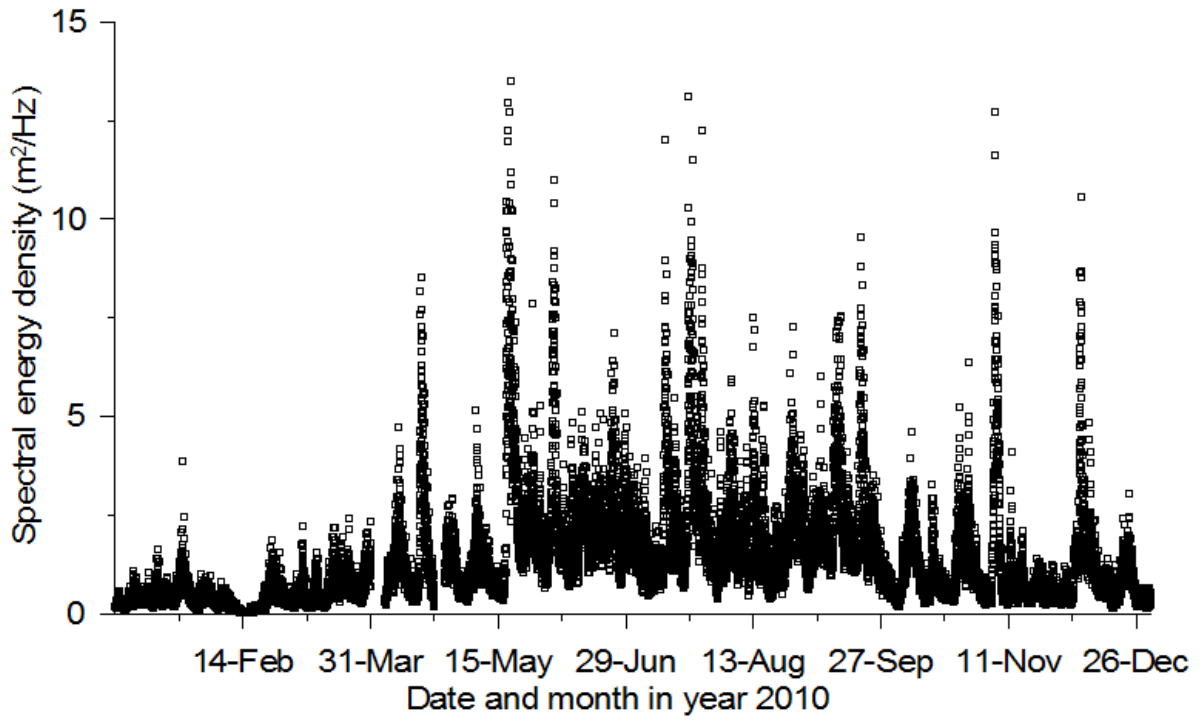


Figure 9 Time history of maximum spectral energy density during 2010

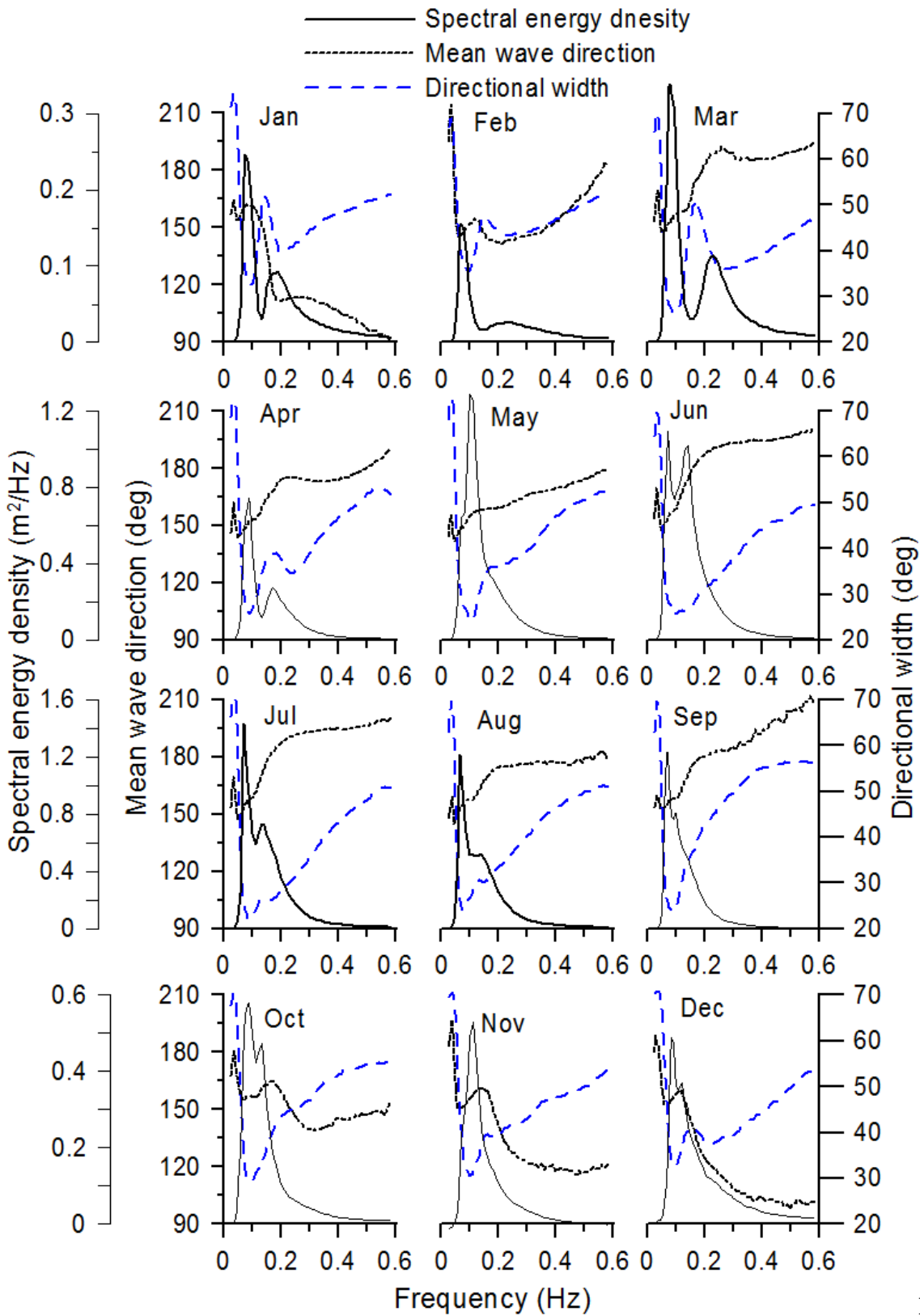


Figure 10 Monthly averaged wave spectra (solid line), mean wave direction (dashed line) and directional width (dotted line) in different months

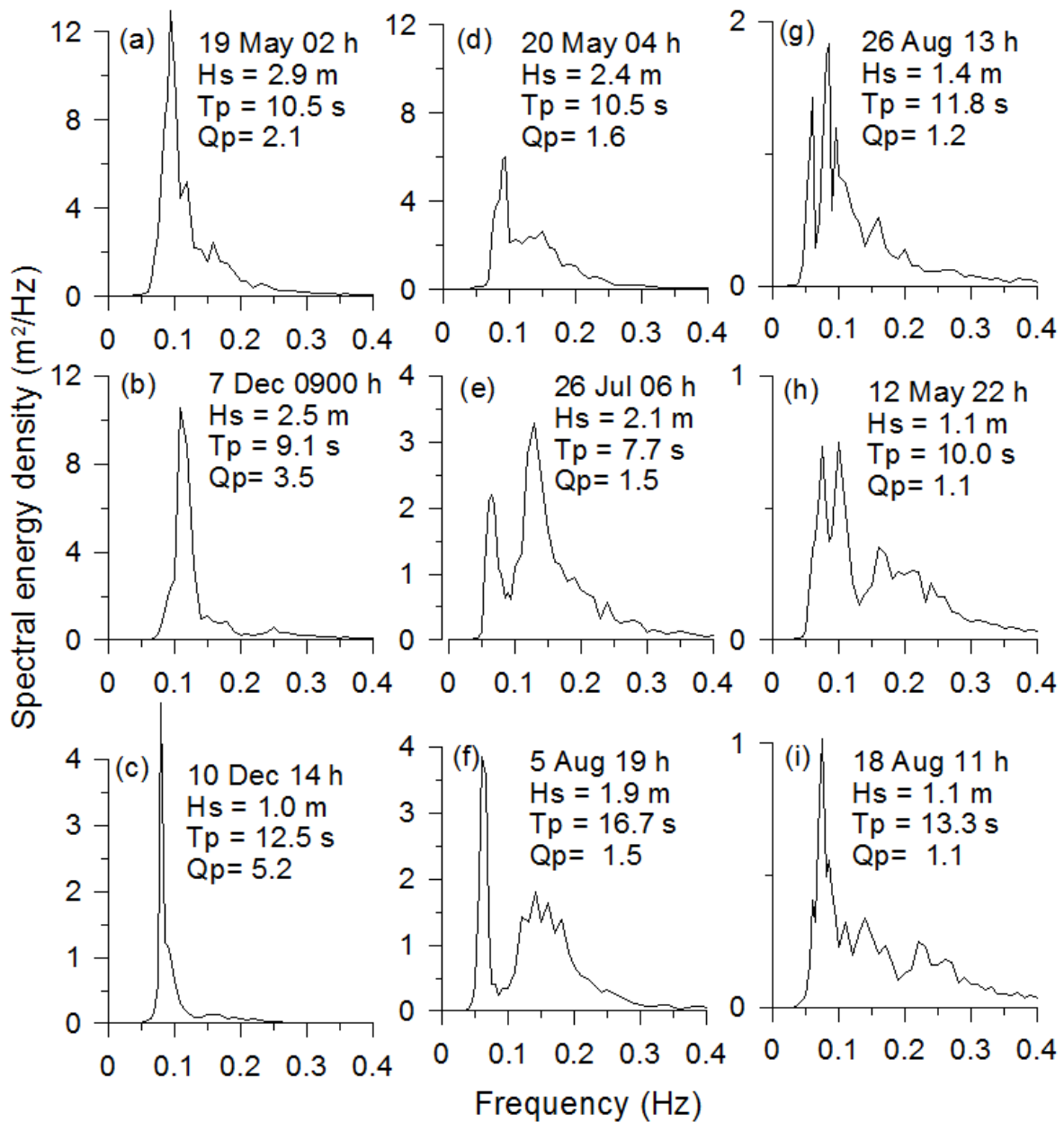


Figure 11 Typical single and multi-peaked wave spectra recorded

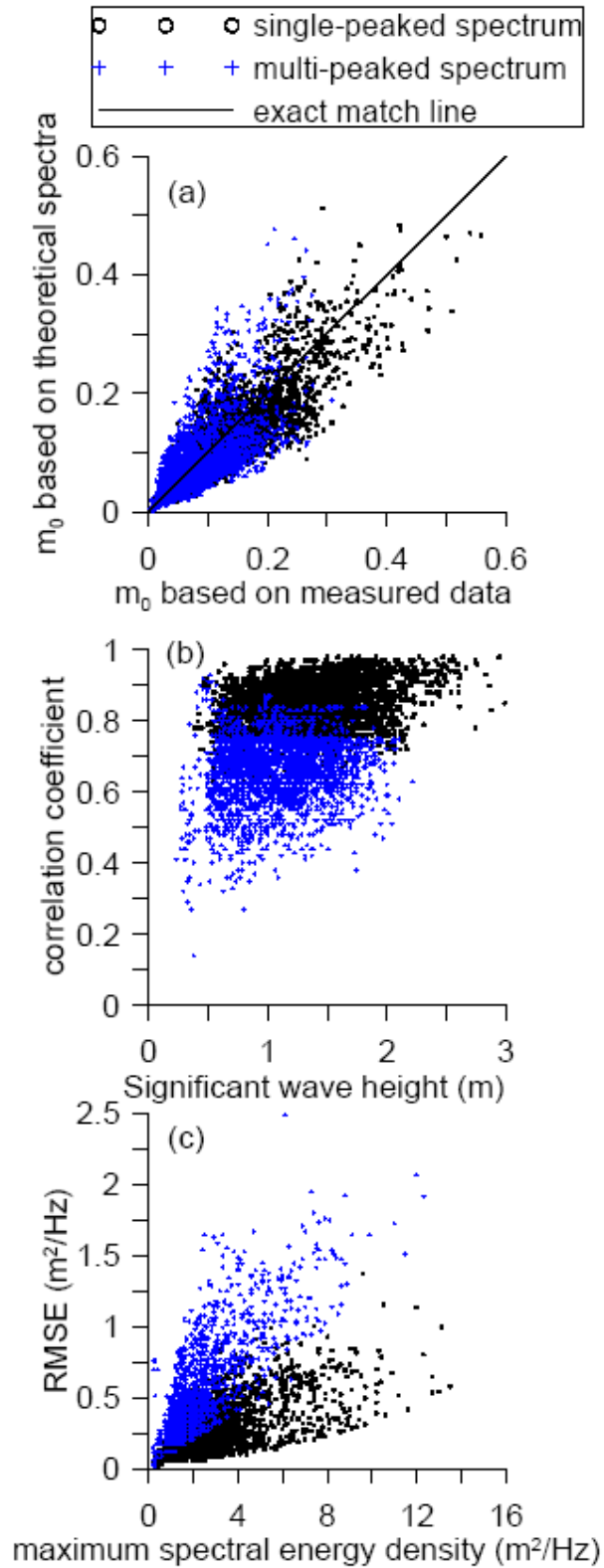


Figure 12. Variation of (a) zeroth spectral moment estimated based on measured and theoretical spectra, (b) correlation coefficient between measured and theoretical spectra with significant wave height and (c) root mean square error with maximum spectral energy density